Supramolecular Self-Assembly of Architecturally Variant α-Cyclodextrin Inclusion Complexes as Building Blocks of Hexagonally Aligned Microfibrils

Jae Woo Chung, Tae Jin Kang, and Seung-Yeop Kwak*

School of Materials Science and Engineering, Seoul National University, San 56-1, Sillim-dong, Gwanak-gu, Seoul 151-744, Korea

Received October 30, 2006; Revised Manuscript Received April 6, 2007

ABSTRACT: Inclusion complexes (ICs) were prepared by the host−guest reaction between α-cyclodextrin (α-CD) and four poly(ϵ-caprolactone)s (PCLs) with different molecular architectures: star-shaped PCL (SPCL) with a radial architecture, random branched PCL (RPCL) with a conical architecture, poly(propylene glycol)−PCL block copolymer (PPG−PCL) with a diblock architecture, and PCL−diol (LPCL) with a linear architecture. Then, the ICs were self-assembled by treatment with suitable polar solvent such as THF. From WAXD, it was found that both the ICs and the self-assembled ICs (SA-ICs) obtained from THF treatment of ICs had hexagonally organized channel-type crystalline structure, resulting from inclusion complexation between α-CD and PCL chain. Combined results of WAXD, FE-SEM, and SAXS further revealed that ICs had the microfibril structure in which single IC strands were hexagonally aligned in the horizontal direction. The microfibrils in ICs were then reorganized by THF treatment, thereby developing well-defined supramolecular structure for ICs with RPCL (R−IC), PPG−PCL (P−IC), and LPCL (L−IC), except IC with SPCL (S−IC). From SAXS experiments, it was verified that the self-assembled supramolecular structures were attributed to continuous alignment of the microfibril by THF. Furthermore, SA-ICs with RPCL, PPG−PCL, and LPCL (R−SA-IC, P−SA-IC, and L−SA-IC, respectively) exhibited the different supramolecular structure, depending on the architecture of the respective polymeric guests. In particular, both R−SA-IC and P−SA-IC showed the microphase separated supramolecular structure because of block-selected inclusion complexation of α-CD as confirmed by ^{1}H NMR. However, the radial architecture of SPCL was considered to hinder the continuous packing of microfibril, thereby supramolecular structure being not accomplished in S−SA-IC. Interestingly, the development of the supramolecular structures was found to be obtained only by treatment with the THF among the various polar solvents.

Introduction

Various types of inclusion complex (IC) formed by noncovalent host−guest interaction have been extensively investigated and reported as useful building blocks for constructing supramolecular structures.[1−3] In particular, cyclodextrins (CDs) have been the most intensively studied as host molecules, on account of their good water-solubility and ability to selectively include a wide range of guest molecules.[4] CDs are cyclic oligosaccharides with six (α-), seven (β-), or eight (γ-) glucose units linked by 1,4-α-glucosidic bonds. CDs have a shallow truncated cone shape and a hydrophobic cavity that is apolar relative to the outer surface. The average diameters of the cavities are 4.5 Å for α-CD, 7.0 Å for β-CD, and 8.5 Å for γ-CD,[5,6] while all of the CD torus heights are 7.9 Å.[7] It is known that the CD cavity can act as a host for a great variety of small or long guest molecules, resulting in IC formation.[8−13] ICs are thought to be formed through a combination of van der Waals forces and hydrophobic interactions between the CD cavity and the guest molecules. Hydrogen bonding between the hydroxyl groups situated along the rim of the CD is also an important driving force leading to the formation of stable ICs.[2,14] In addition, the formation of ICs involves the replacement of the high enthalpy water molecules in the apolar CD cavity with apolar guests, resulting in a favorable enthalpy change induced by the hydrophobic interactions.[6] Hence, entropically unfavorable reactions such as the threading of guest molecules into the narrow cavity of the CD can be overcome by the favorable enthalpy change. Particularly, Tonelli et al. reported several important aspects of the nanothreading of polymeric guest to form polymer-CD−ICs. They suggested that electrostatic, van der Waals, and hydrogen-bonding interactions and relief of conformational strain in CDs are not important, while hydrophobic interactions, exclusion of high energy, cavity-bound water, and crystalline packing of host CDs are important in the formation of IC between CD and polymeric guest.[15] The ICs formed by host−guest reactions between CD and various guest molecules can either have cage- or channel-type crystalline structures. In the former crystal structures, the cavity of a CD molecule is blocked off on both sides by adjacent CDs, thereby leading to isolated cavities. In the latter crystalline structures, the CD molecules are stacked on top of each other, where the linearly aligned cavities produce "endless" channels in which guest molecules can be embedded.[16] For polymeric guests with a long chain-like nature, it was found that the CD molecules were threaded along the polymer chain, where the resulting ICs typically formed channel-type crystalline structures.[17] Due to their novel architectures and applications in various fields, CD ICs with polymers have been extensively studied.[18−30] In addition, it is believed that a supramolecular structure based on ICs can produce materials showing novel properties, with potential uses in biological applications.[31−34] However, most investigations have focused on the threading of linear polymeric guests into the cavities of CDs, although supramolecular structures based on ICs have suggested the potential possibility for many applications such as drug delivery.[10−13,16−23] Recently, increasing attention has been paid to the preparation of CD ICs with star-shaped, hyperbranched, or comb-like polymers on

* Corresponding author. Telephone: +82-2-880-8365. Fax: +82-2-885-1748. E-mail: sykwak@snu.ac.kr.

10.1021/ma0625105 CCC: $37.00
Published on Web 05/12/2007

account of their unique molecular architecture.[31,35−38] These studies showed that CD ICs were formed equally well with nonlinear and linear polymers. In addition, Jeong et al. reported the proliferation of hexagonal unit cells of poly(ethylene glycol) (PEG)/α-CD IC on a micrometer scale.[34] They prepared IC between α-CD and linear PEG, and then obtained the hexagonal microfiber with a well-defined three-dimensional self-assembled supramolecular structure by recrystallizing the IC in a specific solvent. Even though it has been found that not only CD can be threaded by various polymeric guests with nonlinear molecular architectures but also IC can be self-assembled in specific solvent, studies on the self-assembly of CD ICs with the nonlinear polymeric guests was hardly found in the literature. Moreover, as far as our knowledge is concerned, there has been no report to discuss the effect of difference in the architecture of the polymeric guests on the self-assembly of ICs.

Here, we report the supramolecular self-assembly of ICs (SA-ICs) composed of α-CD and various poly(ϵ-caprolactone)s (PCLs) with radial, conical, blocked, or linear molecular architecture. The PCLs were synthesized by ring-opening polymerization, and ICs were prepared by the host−guest reaction between α-CD and PCLs. Then, SA-ICs were obtained by the self-assembly of ICs through THF treatment. Finally, the formation and structure of supramolecular self-assembly of architecturally variant α-CD ICs were investigated; thereby, it can be seen that the molecular architecture of the guest molecule and the choice of solvent for self-assembly play an important role in the development of supramolecular structure based on IC.

Experimental Section

Materials. Dipentaerythritol (DPTOL), 2,2-bis(hydroxymethyl)-propionic acid (bis-MPA, 98%), potassium hydroxide (KOH, 99%), benzyl bromide (98%), ϵ-caprolactone (CL, 99%), poly(propylene glycol) monobutyl ether (monobutyl PPG, M_n = ca. 1200), tin(II) 2-ethylhexanoate ($Sn(Oct)_2$, 99%), palladium on activated carbon (Pd/C, 5 wt% palladium), and *p*-toluenesulfonic acid (*p*-TSA, 98.5%) were all purchased from Aldrich Chemical Co. and used as received. α-CD was supplied by Walker-GmbH. *N*,*N*-Dimethylformamide (DMF, 99%), diethyl ether (99%), toluene (99%), methanol (MeOH, 99%), tetrahydrofuran (THF, 99%), acetone (99%), methylene chloride (MC, 99%), and ethyl acetate (EtOAc, 99%) were all purchased from Daejung Chemicals & Metals (Korea) and used without any additional purification. The supplier, Aldrich Chemical Co., informed us that the number-average molecular weight, M_n, of the polycaprolactone diol (LPCL), as a linear counterpart of the star-shaped poly(ϵ-caprolactone) (SPCL), random branched poly(ϵ-caprolactone) (RPCL), and diblock poly-(ϵ-caprolactone) (PPG-PCL) prepared in this study, was 2000.

Measurements. The ^{1}H nuclear magnetic resonance (^{1}H NMR) spectra were recorded at 500 MHz in either $CDCl_3$ or DMSO-d_6 on a Bruker Avance 500 spectrometer. These spectra were used to analyze the chemical structure of the synthesized PCLs and to determine the number of CL units within each branch of the PCL polymer. Stoichiometry of SA-ICs was also obtained by ^{1}H NMR. Gel permeation chromatography (GPC) experiments were performed in order to evaluate the molecular weight of the PCLs using a Waters chromatography system (Waters 1515 HPLC pump, 2414 refractive index detector, and a set of UltraStyragel columns (HR2 + HR4 + HR5)). Wide-angle X-ray diffraction (WAXD) patterns of the PCLs, α-CD, ICs, and SA-ICs were obtained at room temperature on a MAC/Science MXP 18XHF-22SRA diffractometer with a Cu K_α radiation source (wavelength = 0.154 nm). The supplied voltage and current were set to 50 kV and 100 mA, respectively. Powder samples were mounted on a sample holder and scanned at a rate of $2\theta = 5°$ min^{-1} between $2\theta = 5°$ and 40°. The morphologies of the ICs and SA-ICs were visualized by field-emission scanning electron microscopy (FE-SEM, JEOL JSM-6330F). The FE-SEM samples were coated with a thin conductive Pt layer prior to observation. The small-angle X-ray scattering (SAXS) patterns of both ICs and SA-ICs were obtained at room temperature on a Bruker AXS Nanostar with a Cu Kα radiation source (wavelength = 0.154 nm). The supplied voltage and current were set to 40 kV and 35 mA, respectively. A scattering angle range between 0.02 and 2.5°, and a sample-to-detector distance of 106 cm was employed, respectively.

Synthesis of Star-Shaped Poly(ϵ-caprolactone) (SPCL). A six-armed SPCL with a radial architecture was prepared by ring-opening polymerization of CL, which was initiated with DPTOL in the presence of a catalytic amount of $Sn(Oct)_2$. CL (57.05 g, 500 mmol), DPTOL (1.43 g, 5.6 mmol), and $Sn(Oct)_2$ were placed in a reaction flask and polymerization was carried out at 110 °C under dry N_2 for 24 h. The reaction mixture was then cooled to room temperature, dissolved in THF, and then precipitated with an excess of cold methanol. The precipitates were then washed with methanol several times and dried at room temperature in vacuo. (Yield: 90%.) ^{1}H NMR ($CDCl_3$, 300 MHz): δ 3.65 (t, 1H, $-CH_2-$OH of SPCL), 4.06 (t, 13H, $-C(=O)-O-CH_2-$ of SPCL), 2.31 (t, 14H, $-C(=O)-CH_2-$ of SPCL), 1.57−1.70 (m, 28H, $-O-CH_2-\mathit{CH_2}-$ of SPCL), and 1.35−1.43 (m, 14H, $-O-CH_2-CH_2-\mathit{CH_2}-$ of SPCL).

Synthesis of Random Branched Poly(ϵ-caprolactone) (RPCL). RPCL with a conical geometry were synthesized by polycondensation with AB_2-type macromonomers under continuous water removal, as proposed by Kwak et al.[37] (Yield: 90%.) ^{1}H NMR ($CDCl_3$, 300 MHz): δ 3.65 (t, 0.8H, $-CH_2-$OH of RPCL), 4.06 (t, 19H, $-C(=O)-O-CH_2-$ of RPCL), 2.28−2.33 (t, 20H, $-C(=O)-CH_2$ of RPCL), 1.60−1.70 (m, 40H, $-O-CH_2-\mathit{CH_2}-$ of RPCL), 1.35−1.43 (m, 20H, $-O-CH_2-CH_2-\mathit{CH_2}-$ of RPCL), 4.20−4.30 (m, 1H, OH−C(=O)−C($-CH_3$)($-CH_2$)$-\mathit{CH_2}-$O− of RPCL), and 1.20−1.3 (s, 0.8H, OH−C(=O)−C$(-CH_2)_2-\mathit{CH_3}-$ of RPCL). For the preparation of AB_2-type macromonomers, 3.35 g (25.0 mmol) of bis-MPA and 1.46 g (26 mmol) of KOH were dissolved in DMF at 100 °C, and then benzyl bromide (4.47 g, 26 mmol) was added. After 15 h of stirring, the solvent was evaporated and the residue dissolved in 300 mL of diethyl ether and extracted with distilled water. The crude product was purified by recrystallization from toluene (yield: 65%). The ring-opening polymerization of CL (60 g, 520 mmol) was carried out at 110 °C for 24 h, which was initiated by the hydroxyl groups of the above purified crude product using a catalytic amount of $Sn(Oct)_2$. The product was precipitated in cold MeOH, and then hydrogenated in a mixed solvent of THF/EtOAc (20/80, v/v) with Pd/C (10 wt %) under a hydrogen (H_2) atmosphere for 24 h. The Pd/C was removed by filtration and the filtrate was concentrated by rotary evaporation. The concentrated filtrate was then poured into cold MeOH to precipitate the AB_2-type PCL macromonomer as a white solid (yield: 90%). ^{1}H NMR ($CDCl_3$, 300 MHz): δ 3.65 (t, 1H, $-CH_2-$OH of AB_2-type macromonomer), 4.06 (t, 16H, $-C(=O)-O-CH_2-$ of AB_2-type macromonomer), 2.31 (t, 17H, $-C(=O)-CH_2$ of AB_2-type macromonomer), 1.59−1.70 (m, 34H, $-O-CH_2-\mathit{CH_2}-$ of AB_2-type macromonomer), 1.28−1.43 (m, 17H, $-O-CH_2-CH_2-\mathit{CH_2}-$ of AB_2-type macromonomer), 4.25 (s, 0.8H, OH−C(=O)−C($-CH_3$)($-CH_2$)$-\mathit{CH_2}-$O− of AB_2-type macromonomer), and 1.28 (s, 0.6H, OH−C(=O)−C$(-CH_2)_2-CH_3-$ of AB_2-type macromonomer).

Synthesis of Poly(propylene glycol)-*b*-Poly(ϵ-caprolactone) (PPG—PCL). A PPG−PCL diblock copolymer was prepared by the ring-opening polymerization of CL, which was initiated using the terminal hydroxyl groups of monobutyl PPG in the presence of a catalytic amount of $Sn(Oct)_2$. The preparation of PPG−PCL was carried out as follows. CL (57.05 g, 500 mmol), monobutyl PPG (40 g, 33.3 mmol), and $Sn(Oct)_2$ were first placed in a reaction flask, and then polymerized at 110 °C under dry N_2 for 24 h. The mixture was then cooled to room temperature, dissolved in THF, and precipitated with an excess of cold methanol. The precipitates were washed several times with methanol and dried at room temperature in vacuo. (Yield: 90%.) ^{1}H NMR ($CDCl_3$, 300 MHz): δ 3.65 (t, 1H, $-CH_2-$OH of PPG−PCL), 4.06 (t, 15H, $-C(=O)-O-CH_2-$ of PPG−PCL), 3.51−3.57 (m, 8H, −O−

Scheme 1. Synthesis Routes of SPCL, RPCL, and PPG-PCL

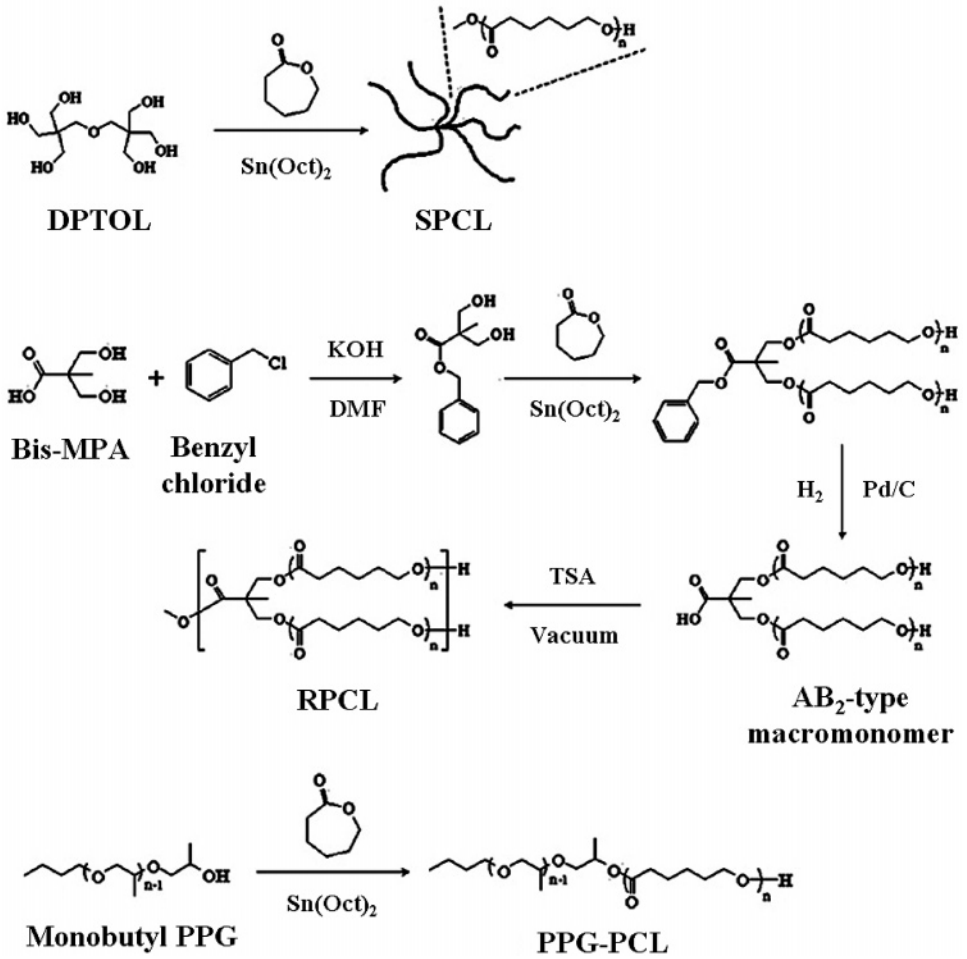

CH$_2$−CH(−CH$_3$)− of PPG−PCL), 3.39−3.42 (m, 5H, −O−CH$_2$−*CH*(−CH$_3$)− of PPG−PCL), 2.31 (t, 15H, −C(=O)−CH$_2$ of PPG−PCL), 1.60−1.70 (m, 30H, −O−CH$_2$−*CH*$_2$− of PPG−PCL), 1.35−1.43 (m, 15H, −O−CH$_2$−CH$_2$−*CH*$_2$− of PPG−PCL), 1.25 (m, 0.4H, CH$_3$−CH$_2$−*CH*$_2$−CH$_2$−O−), 1.20 (m, 0.4H, CH$_3$−*CH*$_2$−CH$_2$−CH$_2$−O−), 1.14 (m, 13H, −O−CH$_2$−CH(−*CH*$_3$)− of PPG−PCL), and 0.90 (m, 0.6H, *CH*$_3$−CH$_2$−CH$_2$−CH$_2$−O−).

Preparation of Supramolecular Self-Assemblies of Inclusion Complex (SA-ICs). The SA-ICs were prepared as follows; α-CD (10 g, 10 mmol) was dissolved in distilled water (75 mL) at 60 °C. SPCL (1.3 g, 0.1 mmol), HPCL (2.0 g, 0.14 mmol), PPG−PCL (3.0 g, 0.5 mmol), and LPCL (1 g, 0.5 mmol) were dissolved in 20 mL of acetone, respectively. Then, PCL solutions were added dropwise to the α-CD solution at 60 °C with vigorous stirring for 24 h. The resulting mixtures were cooled to room temperature and further stirred for 24 h. The precipitated products, i.e., ICs were collected by filtration, and washed with distilled water and acetone to remove free α-CD and PCLs. The ICs were dried overnight in vacuo, and then vigorously stirred in THF for a few hours to trigger the SA-ICs. The dispersed products (SA-ICs) in THF were collected by filtration and dried overnight in vacuo (Yield: 50−65%). The ICs of with SPCL, RPCL, PPG−PCL, and LPCL are referred to herein as S−IC, R−IC, P−IC, and L−IC, respectively, and the SA-ICs obtained from THF treatment of S−IC, R−IC, P−IC, and L−IC are denoted as S−SA-IC, R−SA-IC, P−SA-IC, and L−SA-IC, respectively.

Results and Discussion

Synthesis of PCLs with Different Molecular Architectures. PCLs with different molecular architectures (SPCL, RPCL, and PPG−PCL) were successfully prepared by the ring-opening polymerization of CL triggered by the hydroxyl groups of DPTOL, bis-MPA, and monobutyl PPG, respectively. As shown in the synthetic routes of Scheme 1, SPCL has a radial geometry consisting of six arms (bearing multifunctional hydroxyl groups) that extend from the SPCL core. RPCL consisting of three AB$_2$-type PCL macromonomer having two hydroxyl end groups has a fanwise conical shape with four PCL branching chains spreading from the core, as verified by Choi and Kwak.[39] PPG−PCL is a block copolymer consisting of PPG and PCL chains with a linear shape. The average number of CL units per branch of SPCL and PPG−PCL was calculated from the integral ratio between the −CH$_2$− peak corresponding to $\delta = 2.3$ and the −CH$_2$OH peak corresponding to $\delta = 3.6$. For RPCL, the

Table 1. Synthesis Results of SPCL, RPCL, and PPG−PCL Polymerized Using the Hydroxyl-Containing Initiator and Sn(Oct)$_2$ at 110 °C for 24 h

sample	[M]/[I][b]	$M_{n,GPC}$ (g/mol)	PDI$_{GPC}$[c]	no. of CL/branches	no. of terminal hydroxyls
SPCL	89/1	13 000	1.2	14	6
RPCL	31/1	14 000	1.5	17	4[d]
PPG−PCL	15/1	4000	1.3	15	1
LPCL[a]		2000		17	2

[a] Product purchased from Aldrich. [b] M = CL, I = hydroxyl containing initiator. [c] Polydispersity index determined by GPC. [d] The number of terminal hydroxyl groups of RPCL can be estimated from the average number of AB$_2$-type macromonomers in RPCL acquired by the following equation:[37] $\langle N_{AB_2}\rangle = m/2\langle N_{CL}\rangle - m$. $\langle N_{AB_2}\rangle$: The average number of AB$_2$-type macromonomers in RPCL. $\langle N_{CL}\rangle$: The average number of CL/branches in AB$_2$-type macromonomers. *m*: The ratio of the integrated area of −CH$_2$− peaks corresponding to $\delta = 2.3$ to that of −CH$_2$OH peaks corresponding to $\delta = 3.6$ in RPCL.

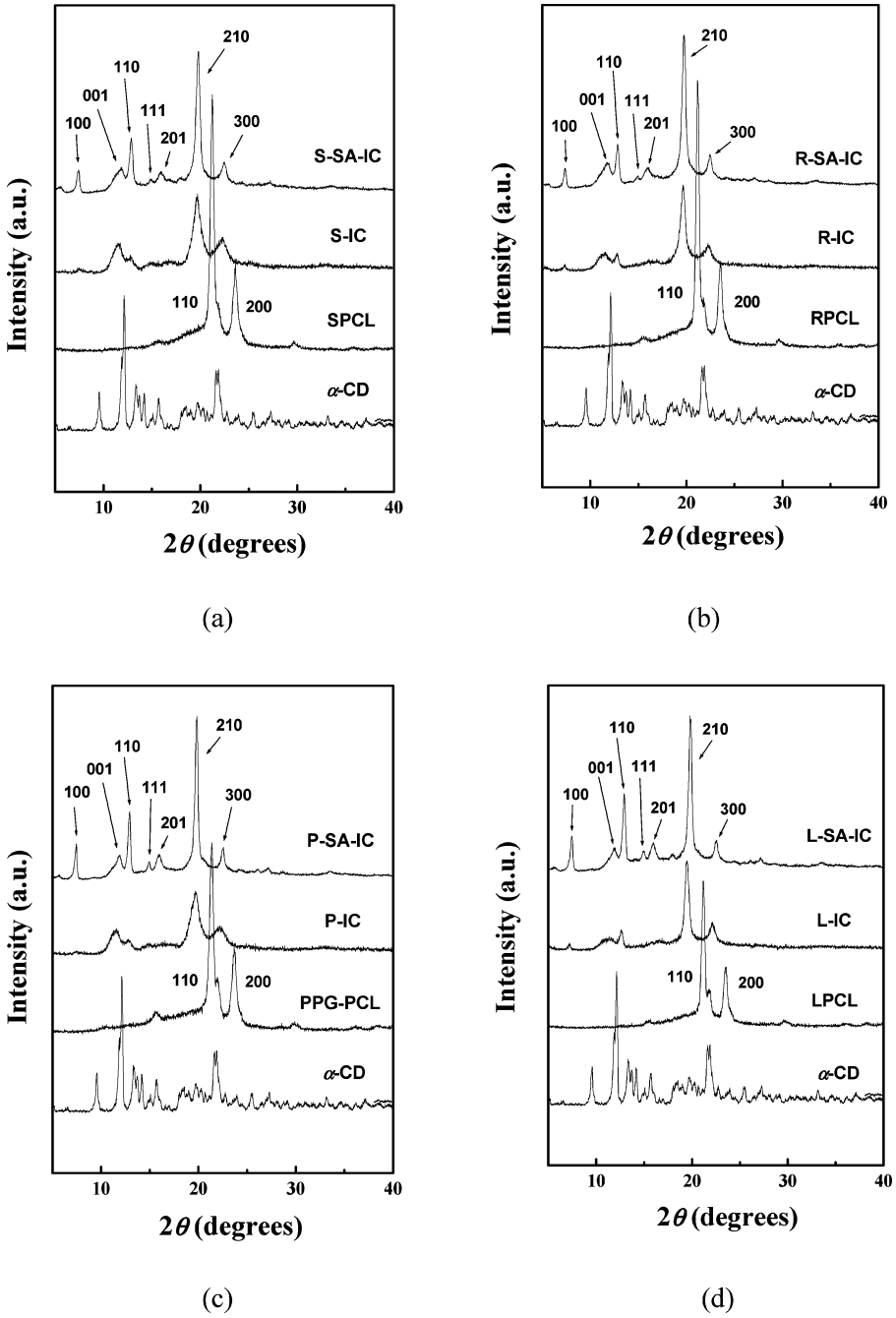

Figure 1. WAXD patterns of α-CD, PCLs, ICs, and SA-ICs.

average number of CL units per branch was determined from the integral ratio between the $-CH_2-$ peak corresponding to $\delta = 2.28-2.33$ and the $-CH_2OH$ peak corresponding to $\delta = 3.6$ in the AB_2-type macromonomer. As shown in Table 1, the average numbers of CL units per branch of SPCL, RPCL, and PPG−PCL were ca. 14, 17, and 15, respectively. This indicates that SPCL, RPCL, and PPG−PCL had similar branching chain lengths as a result of controlling the molar ratio between the CL units and initiators. The average number of CL units in LPCL, which was used as a linear counterpart of SPCL, RPCL, PPG−PCL, was 17. The detailed results are summarized in Table 1.

Inclusion Structure of Self-Assembled Inclusion Complexes (SA-ICs). By adding each SPCL, RPCL, PPG−PCL, and LPCL solution to a saturated aqueous solution of α-CD, it was possible to obtain precipitated products, implying occurrence of the inclusion complexation between α-CD and PCLs.[28] Then, all the precipitates, i.e., inclusion complexes (ICs), were further treated with a specific polar solvent such as THF to form the self-assembled inclusion complexes (SA-ICs) with supramolecular structure. FT-IR spectra showed that the C═O stretching band of PCL (1725 cm^{-1}) was shifted to a higher frequency (1736 cm^{-1}) in the spectra of the SA-ICs (Supporting Information: Figure S-1). DSC exhibited that the peak corresponding to the melting of the PCL block disappeared for SA-ICs (Supporting Information: Figure S-2) and TGA showed that SA-ICs had higher decomposition temperatures relative to free α-CD (Supporting Information: Figure S-3). These results indicate that α-CD was stably complexed with a single PCL chain and there were no free PCLs present in the SA-ICs.[27,40−41] Figure 1 shows the WAXD patterns observed for α-CD, PCLs, ICs, and SA-ICs. The major peaks at 9.6, 12.1, 13.3, 14.1, 15.7, and 21.7° were observed for the α-CD. The WAXD patterns of the PCLs showed prominent peaks at ca. 21.3 (110) and 23.6°

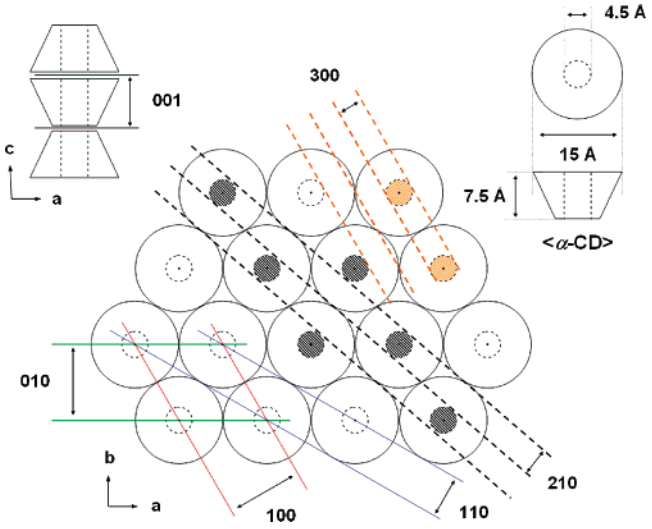

Figure 2. Schematic illustration of channel-type crystalline structure (or microfibril structure) of both ICs and SA-ICs, which is determined from theoretical calculations. This predicted structure is in good agreement with the experimental results obtained from WAXD.

Table 2. Stoichiometric Results of S−ICs and SA-ICs

sample	stoichiometry[a]	average no. of threaded CDs / branches	length of included block (nm)/branches
S−SA-IC (S−IC)	2.21 (2.18)	6.5	4.9
R−SA-IC (R−IC)	1.50 (1.50)	17[b]	12.8[c]
P−SA-IC (P−IC)	0.81 (0.80)	18.7	14.0
L−SA-IC (L−IC)	1.09 (1.08)	15.5	11.6

[a] CL/CD. [b] Average number of CDs threaded on an end branching single PCL chain extended from branching point of RPCL. [c] Average length of CD block presented on an end branching single PCL chain extended from branching point of RPCL.

(200), indicating a body-centered orthorhombic crystalline structure. However, the diffractograms of the ICs and the SA-ICs showed the pattern that is quite deviated from those of the α-CD and PCLs. Prominent peaks observed at ca. 7.6 (100), 12.8 (110), and 19.6° (210) were explained as resulting from the hexagonal unit cell, as reported for α-CD IC with PEG,[36] while the major crystalline peaks for the PCLs were notably absent. Moreover, the diffractograms of both ICs and SA-ICs showed a strong (210) reflection, suggesting a channel-type crystalline structure due to the long-chain nature of PCLs.[21,29,36,42−44] Thus, it was considered that α-CDs were closely packed along a PCL chain in the vertical direction (so-called "single IC strand") and single IC strands were hexagonally aligned in the horizontal direction, as schematically illustrated in Figure 2. In addition, this structure was all observed in the ICs and the SA-ICs, regardless of types of PCL architecture. However, SA-ICs showed somewhat narrower and more vivid peaks than ICs, indicating the increase in the crystalline size and the regularity of crystalline structure. ^{1}H NMR (Supporting Information: Figure S-4) indicated that SA-ICs had the difference of the inclusion formation depending on the PCL architecture. Stoichiometry (CL/CD) of the SA-ICs was evaluated by the molar ratio of the monomeric repeating unit of PCLs to α-CD acquired from ^{1}H NMR spectra. As seen in Table 2, a stoichiometry of 1.09 was determined for L−SA-IC, which implied that a α-CD molecule was bound to a single CL unit and the α-CDs were almost close-packed from one end of the LPCL chain to the other.[45] Thus, given that the average number of repeat units in LPCL was 17, the stoichiometric value suggests that 15.5 α-CD could be threaded by LPCL (0.75 nm × 15.5 = 11.6 nm). For S−SA-IC, the corresponding stoichiometry, 2.21, was higher than that of L−SA-IC. This indicates that 6.5 α-CDs were threaded in each branching arm of SPCL, which was ascribed to the steric hindrance by the dense branching architecture around core of SPCL.[31,32,35,46] A stoichiometry of 1.50 was observed for R−SA-IC. Considering the architecture of RPCL, the value of 1.50 is explained by the fact that α-CDs are only close-packed on the end branching chain extended from branching point of RPCL because α-CDs do not pass through branching point in RPCL. On the other hand, the stoichiometric value of P−SA-IC was less than 1, suggesting that not only α-CDs were present in the PCL block but also a few of them may also be present in the PPG block; the latter is somewhat contrary to the previous reports which inferred that α-CDs do not include PPG.[13,40,47] Thus, S−SA-IC, R−SA-IC, and P−SA-IC are considered to have the separated domains consisting of complexed and uncomplexed component as polymer-*block*-polypseudorotaxanes (Figure 3) due to the block-selected inclusion complexation of α-CD depending on the architecture of PCLs.

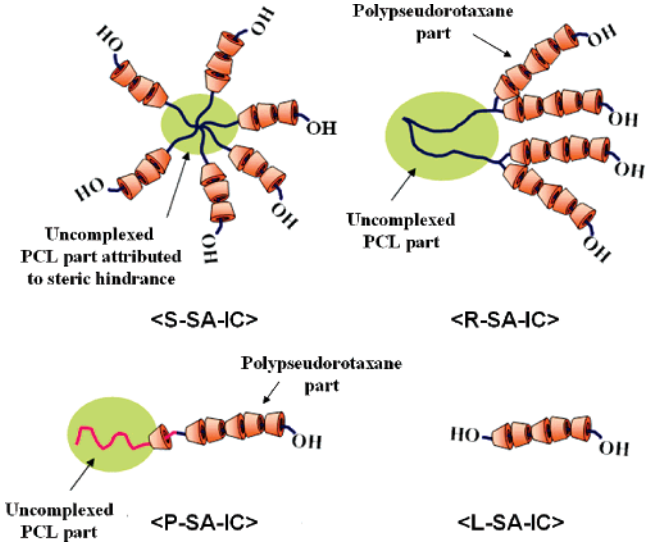

Figure 3. Schematic illustrations of the inclusion formation of SA-ICs.

Supramolecular Structure of Self-Assembled Inclusion Complexes (SA-ICs). To observe the solid-state morphological difference between ICs and SA-ICs, FE-SEM experiments were carried out. Figure 4 is FE-SEM images of S−IC, R−IC, P−IC, and L−IC. The ICs showed very rough surface morphology, while α-CD exhibited a formation of primary domain ascribed to the aggregation of α-CDs and PCLs revealed the smooth surface morphologies. (Supporting Information: Figure S-5) Besides, it was rather difficult to reveal any specific ordered morphologies, despite the hexagonally aligned IC strands (in Figure 2) were verified to be present in ICs by WAXD. On the other hand, the morphologies of the SA-ICs formed from THF treatment were quite different from those of ICs. In Figure 5, all of the SA-ICs exhibited the formation of hexagonally well-defined supramolecular structure on a micrometer scale with the exception of S−SA-IC; the morphology of S−SA-IC was shown to be very rough similar as that of S−IC. In order to clarify these morphological differences in more detail, SAXS experiments were carried out, resulting in Figure 6 as intensity plots against scattering vector, q, for both ICs and SA-ICs. In Figure 6, all the ICs showed nonlinear decay of scattering intensity at the range of q below ~0.04 Å^{-1} for S−IC and ~0.03 Å^{-1} for R−IC, P−IC, and L−IC, presenting data indicative of

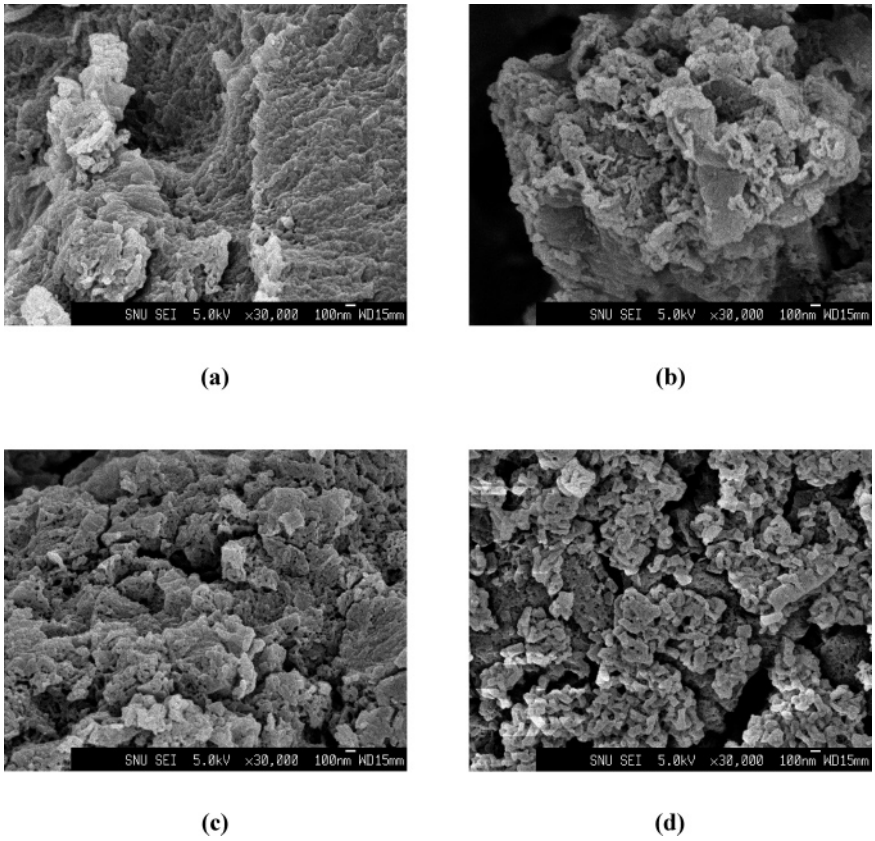

Figure 4. FE-SEM images of ICs: (a) S−IC, (b) R−IC, (c) P−IC, and (d) L−IC.

a broad scattering peak. This indicated that structural scattering units corresponding to the size below about 15 nm for S−IC and 20 nm for R−IC, P−IC, and L−IC were present in a disordered state. Considering the existence of hexagonally ordered IC strands in ICs as shown in WAXD results, these scattering units in ICs were considered to be attributed to the formation of the microfibril structure in which IC strands were hexagonally packed in some extent. Moreover, it was considered that broad scattering peaks of ICs in SAXS were ascribed to the random aggregation of the microfibril. However, scattering intensity of SA-ICs followed linear decay and the broad scattering peak observed in ICs disappeared, with the exception of S−SA-IC. This implied that structural boundary between the microfibrils in ICs became no more distinguishable for R−SA-IC, P−SA-IC, and L−SA-IC on account of developing of supramolecular structure by means of continuous packing of the microfibril as building blocks. Thus, morphological structure (Figure 5) of SA-ICs differed from those of ICs on a microscale, despite WAXD showed that both ICs and SA-ICs had the same crystalline structure on a nanoscale. On the other hand, S−SA-IC showed a similar pattern of scattering intensity decay as S−IC, indicating that distinguishable structural boundaries between microfibrils in S−IC were still maintained in S−SA-IC, even after self-assembly treatment with THF. This was due to the fact that continuous packing of microfibrils was not accomplished and supramolecular structure was not developed in S−SA-IC because of the radial architecture and geometrical constraints of SPCL. In fact, Jeong et. al have reported the proliferation of hexagonal unit cells of poly(ethylene glycol) (PEG)/α-CD IC on a micrometer scale in a specific solvent.[34] They prepared PEG/α-CD IC from α-CD and linear PEG and then obtained the hexagonal microfiber with a well-defined three-dimensional self-assembled supramolecular structure by recrystallizing the PEG/α-CD IC in phosphate buffer solution. However, they did not clearly discuss the reorganization process of PEG/α-CD IC. In addition, they did not show the effect of the architecture of the polymeric guests on self-assembly of IC. In order to explain the reorganization process of solid-state morphology observed in SA-ICs, two possible mechanisms were hypothesized: one was the rearrangement of the single IC strands and the other was the reorganization of the microfibrils. Generally, when a polymeric guest is included into the α-CD cavity, a number of hydrogen bonds are established between the hydroxyl groups situated along the rim of the α-CD, and these produce large aggregates.[2,14] Hydrogen bonding is the most important driving force to maintain the stable inclusion structure as well as the aggregation structure. In particular, polymeric inclusion compounds are not water-soluble because of hydrogen-bonding network formation, but they dissolve in strong polar solvents with dissociation of inclusion structure on account of breaking of hydrogen bonding ascribed to ionization of hydroxyl group in CD.[18,48] If reorganization of solid-state morphology observed in SA-ICs was caused by the rearrangement of the single IC strands, microfibrils in ICs had to be first broken and separated as each single IC strand during THF treatment. This implies the weakening and breaking of the hydrogen bonding formed between single IC strands. If THF has the extent of the strength to break the hydrogen-bonding regularly formed between single IC strands, hydrogen bonding between α-CDs threaded to PCL chain may also be sufficiently broken by THF, resulting in the dissociation of inclusion structure and deth-reading of α-CD from PCL chain. When inclusion structure is dissociated, only α-CD molecule is remained during the sample preparation process such as the filtering after THF treatment because PCL is soluble to THF and CD is insoluble to THF. However, it was confirmed from FT-IR and WAXD that both CD and PCL molecules were present in SA-ICs and the inclusion structure was still maintained in SA-ICs, respectively.

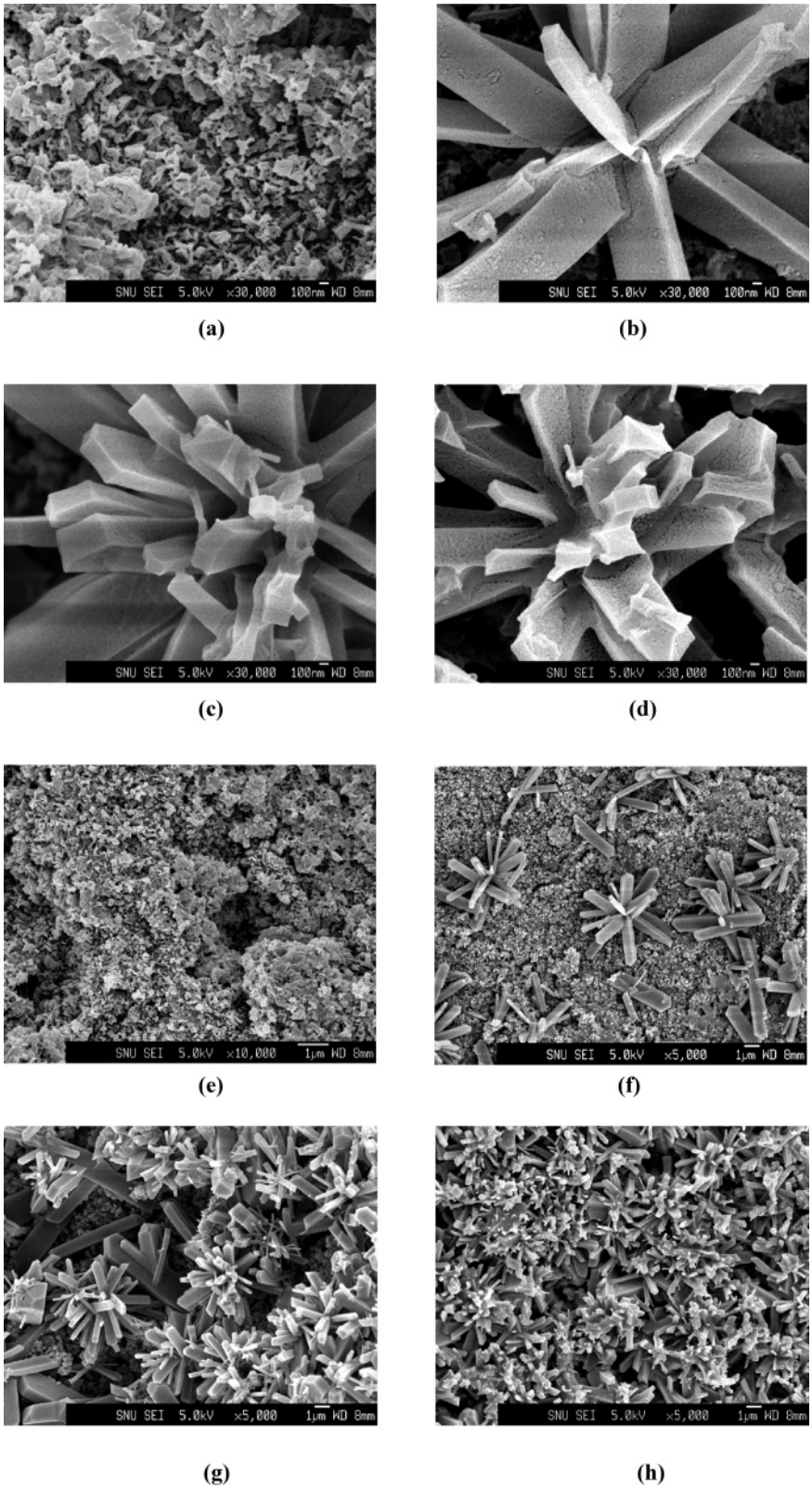

Figure 5. FE-SEM images of the SA-ICs: (a) S−SA-IC (×30 000), (b) R−SA-IC (×30 000), (c) P−SA-IC (×30 000), (d) L−SA-IC (×30 000), (e) S−SA-IC (×10 000), (f) R−SA-IC (×5000), (g) P−SA-IC (×5000), and (h) L−SA-IC (×5000).

This indicates that microfibril structure in ICs was not destroyed during THF treatment. Therefore, it was not considered that reorganization of solid-state morphology observed in SA-ICs was attributed to the rearrangement of the single IC strands. Thus, it is rather reasonable to suggest that proliferation of hexagonal unit observed in solid-state morphologies of SA-ICs is attributed to the reorganization of the microfibril. In the case of the reorganization of the microfibril, the selective breaking of hydrogen bonding by THF is considered as one of the crucial factors to form the self-assembled supramolecular structure observed in SA-ICs. According to above WAXD, SAXS, and FE-SEM results, all of the ICs are considered to have the microfibrils that were formed by strongly hexagonal packing between single IC strands, and microfibril was randomly

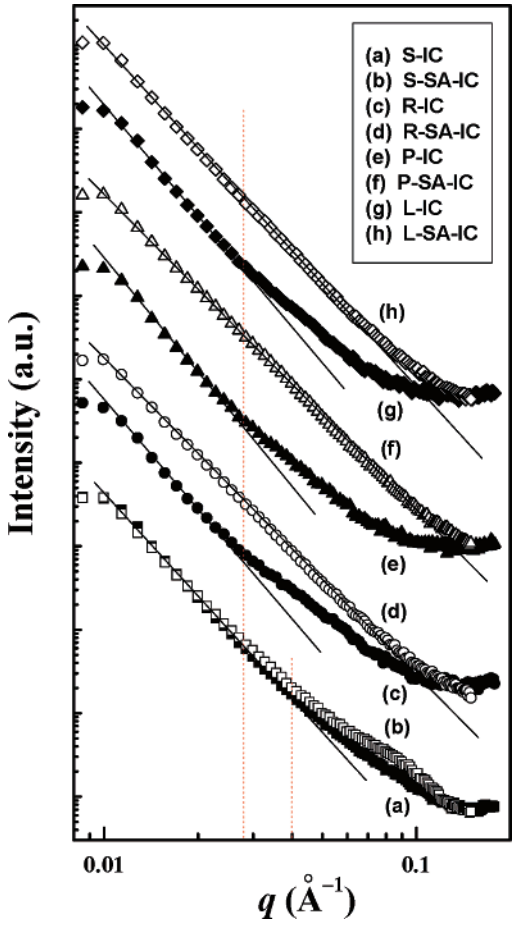

Figure 6. SAXS profiles of ICs and SA-ICs.

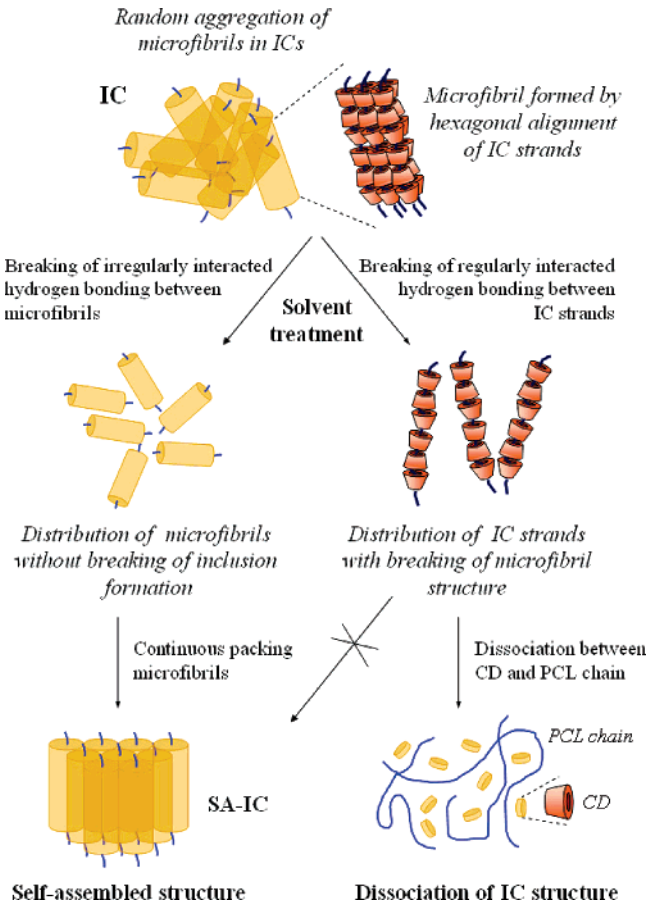

Figure 7. Schematic illustration for self-assembled mechanism of SA-ICs based on the consideration of SAXS results and hypothetical model.

aggregated in ICs. Thus, it seems that THF may not break the regularly arranged hydrogen bonding between single IC strands as well as α-CDs threaded in PCL chain, but hydrogen bonding between microfibrils may be broken by THF due to lower regularity ascribed to the random aggregation of microfibrils, contrary to the regularity of the hydrogen bonding between single IC strands. Thus, the developments of supramolecular structure in R−SA-IC, P−SA-IC, and L−SA-IC may be considered to be attributed to the reorganization of the microfibrils in ICs by THF, and this hypothesis is in good agreement with above SAXS results. A schematic self-assembly process for SA-IC based on the above hypothesis and SAXS results is illustrated in Figure 7.

In addition, self-assembled structure of each R−SA-IC, P−SA-IC, and L−SA-IC exhibited the different supramolecular structure, depending on the architecture of the individual PCL. As shown in Figure 5, R−SA-IC showed some supramolecular structures attributed to the hexagonal alignment of microfibrils, in spite of the presence of the geometrical constraints caused by the branching structure. This can be explained by that R−SA-IC had the lower geometrical constraints relative to S−SA-IC because of the conical geometry and a few branching chains of RPCL. Low geometrical constraints can be sufficiently collapsed by intermolecular hydrogen bonding between the α-CD component in R−SA-IC.[33] In addition, P−SA-IC and L−SA-IC showed the formation of a greater number of supramolecular structures than R−SA-IC, on account of the linear architecture of the these PCLs, which is not affected by geometrical constraints. However, a less hexagonally packed structure was clearly observed for P−SA-IC compared to L−SA-IC, which might be attributed to the uncomplexed PPG component in P−SA-IC hindering the formation of an arranged supramolecular structure. Meanwhile, both R−SA-IC and P−SA-IC had smooth surfaces (Figure 5), whereas L−SA-IC was found to have a rough surface morphology. This result implies the occurrence of microphase separation between the complexed and uncomplexed components in R−SA-IC and P−SA-IC by THF. From the above stoichiometric results obtained from ^{1}H NMR, it was found that both R−SA-IC and P−SA-IC had a polymer-*block*-polypseudorotaxane structure attributed to the branching point of RPCL and greater PPG chain thickness relative to the diameter of the α-CD cavity, respectively. Thus, it is considered that the complexed components (not soluble with THF) in R−SA-IC and P−SA-IC were aggregated toward the interior to prevent their exposure to the THF, while the uncomplexed components (soluble with THF) of R−SA-IC and P−SA-IC were extended toward THF. These differences of solvophobicity between complexed and uncomplexed components in THF may cause microphase separation and result in smooth surface morphologies of R−SA-IC and P−SA-IC. Structures of SA-IC based on the above FE-SEM and SAXS results were schematically illustrated in Figure 8. Interestingly, the SA-ICs to give an ordered supramolecular morphology were found in only THF. Acetone, MC, MeOH, DMF, and DMSO treatment failed to produce the hexagonally packed morphology.

From the combined results of WAXD, SAXS, and FE-SEM, it is believed that self-assembled structure observed in SA-ICs is attributed to the recrystallization of microfibril randomly aggregated in IC. Moreover, our results show that architecture of polymeric guest affects the reorganization of solid-state morphology observed in SA-ICs. To the best of our knowledge,

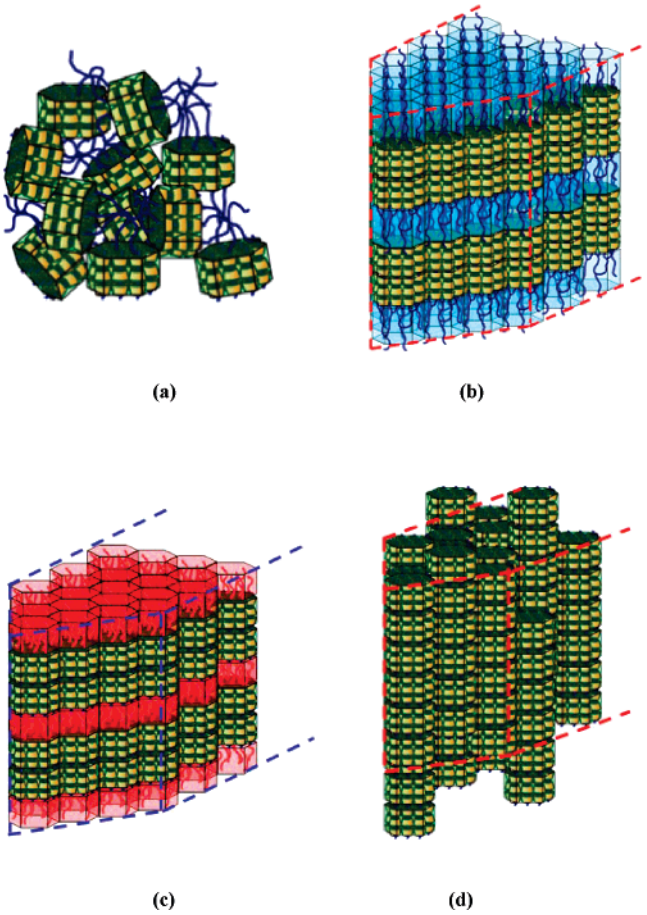

Figure 8. Schematic illustration for supramolecular structure of the SA-ICs based on WAXD, FE-SEM, and SAXS results: (a) S−SA-IC, (b) R−SA-IC, (c) P−SA-IC, and (d) L−SA-IC.

this is the first detailed report that investigates the effect of various polymeric architectures on the formation of supramolecular structure of IC by using suitable solvent treatment.

Conclusions

α-CD SA-ICs with four types of PCLs having distinct molecular architectures—SPCL (radial), RPCL (conical), PPG−PCL (diblock), and LPCL (linear)—were successfully prepared by the reorganization of the initially formed ICs when exposed in THF. It was found that both ICs and SA-ICs had a hexagonally channel-type crystalline structure attributed to inclusion complexation between α-CD and PCL chain, irrespective of the PCL molecular architecture. However, S−SA-IC, R−SA-IC, and P−SA-IC had a polymer-*block*-polypseudorotaxanes type structure depending on the architecture of PCL, because of block-selected inclusion complexation of α-CD. From WAXD, FE-SEM, and SAXS, it was confirmed that ICs had the microfibril structure attributed to hexagonal packing of some IC strands. The microfibril in ICs was reorganized by THF treatment, and then well-defined supramolecular structure on microscale was developed from each IC due to the continuous packing of hexagonally shaped microfibrils, excepting S−IC. However, no supramolecular structure was observed in S−SA-IC because of the radial structure of SPCL. This result was in good agreement with the SAXS result. Additionally, individual supramolecular structure constructed in R−SA-IC, P−SA-IC, and L−SA-IC depends on the architecture of PCL. In particular, R−SA-IC and P−SA-IC exhibited microphase separation due to polymer-*block*-polypseudorotaxanes attributed to the architecture of PCL. Interestingly, the self-assembled structure of IC was only found to form in THF. Therefore, considering all of the observations described above, it can be thought that the molecular architecture of the guest molecule and the choice of solvent for self-assembly play an important role in formation of the supramolecular self-assembly based on IC.

Acknowledgment. The authors of this paper would like to thank the Korea Science and Engineering Foundation (KOSEF) for sponsoring this research through the SRC/ERC Program of MOST/KOSEF (R11-2005-065).

Supporting Information Available: Fourier transform infrared (FT-IR) spectra in Figure S-1 were recorded on a Perkin-Elmer Spectrum GX spectrometer at frequencies ranging from 400 to 4000 cm^{-1}. Differential scanning calorimetry (DSC) analysis in Figure S-2 was performed using a TA Instruments DSC 2920 under N_2 flow. All of the SA-ICs were first heated from 0 to 100 °C at 20 °C/min to erase the thermal history, then cooled to 0 °C at 20 °C/min, and finally heated to 100 °C at 20 °C/min. Thermogravimetric analysis (TGA) scan data in Figure S-3 was obtained using a TA Instruments TGA 2050 thermal analyzer from room temperature to 600 °C at a heating rate of 10 °C/min under N_2 flow. ^{1}H nuclear magnetic resonance (^{1}H NMR) spectra in Figure S-4 were recorded at 500 MHz in DMSO-d_6 on a Bruker Avance 500 spectrometer, and morphologies of α-CD and PCLs in Figure S-5 were visualized by field-emission scanning electron microscopy (FE-SEM, JEOL JSM-6330F). This material is available free of charge via the Internet at http://pubs.acs.org.

References and Notes

(1) Harada. A. *Coord. Chem. Rev.* **1996**, *148*, 115.
(2) Ceccato, M.; Lo Nostro, P.; Baglioni, P. *Langmuir* **1997**, *13*, 2436.
(3) Herrmann, W.; Keller, B.; Wenz, G. *Macromolecules* **1997**, *30*, 4966.
(4) Wenz, G. *Angew. Chem., Int. Ed. Engl.* **1994**, *33*, 803.
(5) James, W. J.; French, D.; Rundle, R. E. *Acta Crystallogr.* **1959**, *12*, 385.
(6) Bender, M. L.; Komiyama, M. *Cyclodextrin Chemistry*; Springer-Verlag: Berlin, 1978.
(7) Szejtli, J. *Cyclodextrin Technology*; Kluwer Academic Publisher: Dordrecht, The Netherlands, 1988.
(8) Szejtli, J. *Cyclodextrins and Their Inclusion Complexes*; Akademiai Kiado: Budapest, 1982.
(9) Saenger, W. *Angew. Chem., Int. Ed. Engl.* **1980**, *19*, 344.
(10) Harada, A.; Takahashi, S. *J. Chem. Soc., Chem. Commun.* **1984**, 645.
(11) Colquhoun, H. M.; Stoddard. J. F.; Williams, D. J. *Angew. Chem., Int. Ed. Engl.* **1986**, *25*, 487.
(12) Harada, A.; Kamachi, M. *Macromolecules* **1990**, *23*, 2821.
(13) Harada, A.; Kamachi, M. *J. Chem.* Soc. *Chem. Commun.* **1990**, 1322.
(14) Miyake, K.; Yasuda, S.; Harada, A.; Sumaoka, J.; Kimiyama, M.; Shigekawa, H. *J. Am. Chem.* Soc. **2003**, *125*, 5080.
(15) Rusa, C. C.; Rusa, M.; Peet, J.; Uyar, T.; Fox, J.; Hunt, M. A.; Wang, X.; Balik, C. M.; Tonelli, A. E. J. *Inclus. Phenom. Macrocycl. Chem.* **2006**, *55*, 185.
(16) Saenger, W. In *Inclusion Compounds*; Atwood, J. L., Davies, J. E. K., MacNicol, D. D., Eds.; Academic Press: London, 1984; Vol. 2.
(17) Lu, J.; Shin, I. D.; Nojima, S.; Tonelli, A. E. *Polymer* **2000**, *41*, 5871.
(18) Harada, A.; Li, J.; Kamachi, M. *Nature (London)* **1992**, *356*, 325.
(19) Wenz, G.; Keller, B. *Angew. Chem., Int. Ed. Engl.* **1992**, *31*, 197.
(20) Harada, A.; Li, J.; Kamachi, M. *Nature (London)* **1993**, *364*, 516.
(21) Harada, A.; Li, J.; Kamachi, M. *Macromolecules* **1993**, *26*, 5698.
(22) Harada, A.; Li, J.; Kamachi, M. *Nature (London)* **1994**, *370*, 126.
(23) Harada, A.; Li, J.; Kamachi, M. *J. Am. Chem.* Soc. **1994**, *116*, 3192.
(24) Klyamkin, A. A.; Topchieva, I. N.; Zubov, V. P. *Colloid Polym. Sci.*, **1995**, *273*, 520.
(25) Ooya, T.; Mori, H.; Terano, M.; Yui, N. *Macromol. Rapid Commun.* **1995**, *16*, 259.
(26) Born, M.; Ritter, H. *Angew. Chem.* **1995**, *107*, 342.
(27) Noll, O.; Ritter, H. *Macromol. Rapid Commun.* **1997**, *18*, 53.
(28) Huang, L.; Allen, E.; Tonelli, A. E. *Polymer* **1998**, *39*, 4857.
(29) Rusa, C. C.; Tonelli, A, E. *Macromolecules* **2000**, *33*, 1813.
(30) Rusa, C. C.; Luca, C.; Tonelli, A, E. *Macromolecules* **2001**, *34*, 1318.
(31) Zhu, X.; Chen, L.; Yan, D.; Chen, Q.; Yao, Y.; Xiao, Y.; Hou, J.; Li, J. *Langmuir* **2004**, *20*, 484.
(32) He, L.; Huang, J.; Chen, Y.; Liu, L. *Macromolecules* **2005**, *38*, 3351.
(33) He, L.; Huang, J.; Chen, Y.; Xu, X.; Liu, L. *Macromolecules* **2005**, *38*, 3845.

(34) Hwang, M. J.; Bae, H. S.; Kim, S. J.; Jeong, B. *Macromolecules* **2004**, *37*, 8820.
(35) Jiao, H.; Goh, S. H.; Valiyaveettil, S. *Macromolecules* **2002**, *35*, 1980.
(36) Wang, L.; Wang, J.-L.; Dong, C.-M. *J. Polym. Sci.: Part A: Polym. Chem.* **2005**, *43*, 4721.
(37) Huh, K. M.; Ooya, T.; Lee, W. K.; Sasaki, S.; Kwon, I. C.; Jeong, S. Y.; Yui, N. *Macromolecules* **2001**, *34*, 8657.
(38) Sabadini, E.; Cosgrove, T. *Langmuir* **2004**, *37*, 8820.
(39) Choi, J.; Kwak, S.-Y. *Macromolecules* **2003**, *36*, 8630.
(40) Nichio, Y.; Manley, R. St. J. *Polym. Eng. Sci.* **1990**, *30*, 71.
(41) Jiang, S.; Ji, X.; An, L.; Jiang, B. *Polymer* **2001**, *42*, 3901.
(42) Harada, A.; Okada, M.; Li, J.; Kamachi, M. *Macromolecules* **1995**, *28*, 8406.
(43) Huh, K. M.; Ooya, T.; Sasaki, S.; Yui, N. *Macromolecules* **2001**, *34*, 2402.
(44) Li, J.; Li, X.; Zhou, Z.; Ni, X.; Leong, K. W. *Macromolecules* **2001**, *34*, 7236.
(45) Harada, A.; Kawaguchi, Y.; Nichiyama, T.; Kamachi, M. *Macromol. Rapid Commun.* **1997**, *18*, 535.
(46) Chan, S.-C.; Kou, S.-W.; Chang, F.-C. *Macromolecules* **2005**, *38*, 3099.
(47) Okada, M.; Kamachi, M.; Harada, A. *J. Phys. Chem. B* **1999**, *103*, 2607.
(48) Steinbrunn, M. B.; Wenz, G. *Angew. Chem., Int. Ed. Engl.* **1996**, *35*, 2139.

MA0625105